ELSEVIER

Journal of Nuclear Materials 298 (2001) 145–149

journal of nuclear materials

www.elsevier.com/locate/jnucmat

Numerical modelling of glass dissolution: gel layer morphology

F. Devreux *, P. Barboux

Laboratoire de Physique de la Matière Condensée, Ecole Polytechnique & CNRS, 91128 Palaiseau cedex, France

Abstract

Numerical simulations of glass dissolution are presented. The glass is modelized as a random binary mixture composed of two species representing silica and soluble oxides, such as boron and alkali oxides. The soluble species are dissolved immediately when they are in contact with the solution. For the species which represents silica, one introduces dissolution and condensation probabilities. It is shown that the morphology and the thickness of the surface hydration layer (the gel) are highly dependent on the dissolution model, especially on the parameter which controls the surface tension. Simulations with different glass surface area to solution volume ratio (S/V) show that this experimental parameter has important effects on both the shrinkage and the gel layer thickness.

PACS: 81.60 Fs; 82.20 Wt; 82.65 Yh

In a recent paper, we have defined a model for glass dissolution and worked out numerical simulations [1]. The model is based on the consideration of three classes of glass components with different solubilities. *A* species represents silica, *B* corresponds to soluble oxides, such as alkali and boron oxides, and *C* to less-soluble oxides such as Al_2O_3, ZrO_2, Fe_2O_3, rare earth and transuranian oxides. The three components in proportion p_A, p_B and p_C are randomly distributed on a cubic lattice with an initial free interface area of S sites. The composition of the model glass can be related to that of an actual glass by taking into account the chemical coordination of the elements in the glass [1]. In the simulations, the proportion of soluble *B* species was taken in the range 0–25% (it should be kept below the site percolation threshold of the lattice) and that of *C* species in the range 0–15%. *B* elements are dissolved immediately as soon as they stand at the water–glass interface. For *A* and *C* species, one defines dissolution probabilities, which depend on the bonding environment of the element to be dissolved. One also defines condensation probabilities, which are proportional to the concentrations of the species in solution. The *B* solubility and the solution volume V are supposed to be large enough for the dissolved *B* never to condense again.

Our model is closely related to that developed by Aertsens [2–4]. The main difference is that we do not manage explicitly the diffusion of the particles in the solution and within the porous hydration layer. We assume that the diffusion in the liquid phase is very fast with respect to the hydrolysis and condensation reactions of silica. Thus, once dissolved, a particle simply contributes to the (uniform) concentration of the considered species in solution. We also assume that the dissolution of *B* species (boron for example) is much faster than that of *A* species (silica). Finally, we neglect solid state diffusion or interdiffusion. These hypotheses limit the domain of validity of our model to the situations where the whole dissolution is governed by that of silica. This is believed to be the case for the durable nuclear waste glasses in neutral to moderate basic solutions, at least during the main phase of dissolution [5–7]. The main advantage of these simplifications is to save computer time, since managing diffusion is very time-consuming. This allows us to observe the aging of the system long after the saturation of the solution in silica within an acceptable calculation time.

* Corresponding author. Tel.: +33-1 69 33 25 61; fax: +33-1 69 33 30 04.

E-mail address: fd@pmc.polytechnique.fr (F. Devreux).

0022-3115/01/$ - see front matter
PII: S0022-3115(01)00579-7

Within the model defined above, we have studied the behaviour of the system as a function of the proportions of the different elements in glass [1]. Our previous results show that, in the far-from-saturation regime ($S/V = 0$), there is a short initial phase of selective extraction of the soluble B elements. Hereafter, the whole dissolution is limited by that of the A species and one observes the congruent dissolution of A and B. The dissolution rate decreases with the proportion of less-soluble C species and increases strongly with that of soluble B species (more than three orders of magnitude when p_B is changed from 0% to 25%). This is mainly due to the formation of a porous hydrated layer whose thickness increases steeply with p_B. This generates a large active surface area, which speeds up the dissolution process. In the saturation regime ($S/V > 0$), the equilibrium solubility of A species (silica) decreases with the proportion of less-soluble C species, but it is practically independent of that of soluble B species. This is due to the fact that the porous interface between the solid and the solution is practically free of B species. Thus, the mean environment of A species is the same, whatever the initial proportion of B was. After the saturation of the solution, the porous hydrated layer (the 'gel') is rearranged as a result of the dissolution–recondensation dynamic equilibrium. There is a ripening of the pore walls. The pore size gets larger and the porosity is partly occluded. This leads to a reinforcement of the gel layer which becomes protective. The glass rearrangement prevents further extraction of the soluble species beyond the gel layer. In the present paper, we keep the glass composition constant ($p_A : p_B : p_C = 75 : 25 : 0$) and we examine in detail the influence of the dissolution model and that of the experimental S/V parameter on the gel properties.

First-order kinetics is considered to give a good first-approximation description of the dissolution of the silica network [5]. This leads us to write the dissolution rate of the A species as

$$\frac{\mathrm{d}N_A}{\mathrm{d}t} = \sum_i [w_\mathrm{d}(i) - w_\mathrm{c}(i)c_A], \tag{1}$$

where $w_\mathrm{d}(i)$ and $w_\mathrm{c}(i)$ are the dissolution and condensation rate constants and c_A is the A concentration in solution (expressed as a molar fraction). In Eq. (1), the sum runs over all the sites i of the actual surface. In the simplest formulation of the transition state theory, the dissolution and condensation rate constants are independent of the surface site. They are related to the difference in energy between the dissolved state and the condensed state, E_0, through

$$w_\mathrm{d} = w_\mathrm{c} \exp[-E_0/k_\mathrm{B}T]. \tag{2}$$

From Eq. (1), the equilibrium concentration in solution is obtained as: $c_A^{\mathrm{eq}} = w_\mathrm{d}/w_\mathrm{c}$. If one further assumes that the surface area is constant and equal to S, the initial area before alteration, the solution of Eq. (1) is

$$c_A(t) = c_A^{\mathrm{eq}}\left[1 - \exp\left(-\frac{S}{V} w_\mathrm{c} t\right)\right], \tag{3}$$

where V is the solution volume. Eq. (3) implies a scaling of the alteration data with $(S/V) \times t$, which has lead experimentalists to use high S/V ratio to investigate the long-term behaviour. In fact, the situation is more complicated. The actual surface area of the altered glass is not equal to the initial area, the $(S/V) \times t$ scaling is not always obeyed [8], and this simple model misses an essential ingredient – the surface tension – to account for realistic morphology of the altered glass surface.

Eq. (1) with site independent dissolution and condensation rate constants has been simulated for an AB system with $p_A = 0.75$ and $p_B = 0.25$. As most of the experimental tests on nuclear waste glasses are performed at 90°C, where the solubility in silicon is typically in the range 50–200 Si mg/l, $w_\mathrm{d}/w_\mathrm{c}$ is taken equal to 10^{-4} to achieve a realistic solubility (this value corresponds to 10^{-4} Si per water molecule, i.e., 5.5 mmol/l or 150 mg of Si per liter). The initial area is equal to $S = 64 \times 64$ sites and the solution volume to $V = 10^9$ sites, which leads to an S/V ratio of 4×10^{-6}. Taking 0.2 nm as a typical molecular size, this corresponds to 2×10^4 m^{-1}, which is a typical value for the high S/V ratios used in experimental studies [9]. The results of the simulation are given in Figs. 1 and 2. Fig. 1 shows that the A concentration reaches an equilibrium value, as expected from Eq. (3). However, the saturation is obtained much more rapidly than predicted by Eq. (3), since the actual surface area is much larger than the initial surface area. Meanwhile, the B concentration increases linearly without saturation. Fig. 2 displays the evolution of a 64×512 longitudinal cross-section of the sample. One sees that the whole sample is progressively

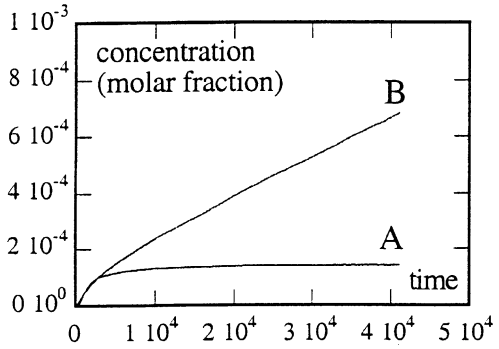

Fig. 1. Evolution of the concentration of A and B particles in solution in the model with site independent dissolution and condensation rate constants. The parameters of the simulation are: $p_B = 0.25$, $w_\mathrm{d} = 10^{-3}$, $w_\mathrm{c} = 10$ and $S/V = 4 \times 10^{-6}$.

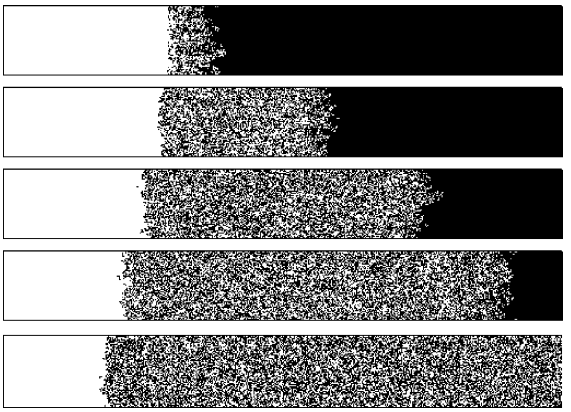

Fig. 2. Evolution of a longitudinal cross-section (64×512) in the model with site independent dissolution and condensation rate constants. The parameters are the same as in Fig. 1. Views at times $t = 10^3, 5 \times 10^3, 10^4, 1.5 \times 10^4$ and 2×10^4.

changed into a swollen foam. The density of this foam is found to be 0.57. As the concentration of A particles in the pristine glass is 0.75, the swelling factor is about 30%. It should be mentioned that the same kind of morphology is obtained when $p_A = 1$ (pure silica). As a consequence of the transformation of the glass in foam, the leaching front progresses endlessly (for an infinite sample) and this causes the B species to be extracted continuously at a rate close to the initial one (Fig. 1). The reason for this behaviour is easy to understand: since surface A species are dissolved without consideration for their bonding environment, there is no surface tension and thus no enthalpic forces to compete with entropy, for which a foam is much better than a monolithic sample. This low-density foam allows soluble species to be extracted without limit. This is an example of non-protective gel. Although such a behaviour may be observed in highly aggressive alkaline leachant, it is not expected in moderate pH conditions (pH $\sim$ 7 to 10), which are the realistic ones for nuclear glasses in disposal environment.

A simple way to introduce surface tension consists in making the dissolution rate constant dependent on the environment of the A atom to be dissolved. We write the stabilization energy of an A particle in the solid state with respect to the dissolved state as $E(i) = E_0 + n_i \Delta E$, where n_i is the number of A–A bonds at site i. Then, $E_0 + \Delta E$ is the stabilization energy for a solid site with only one bond, and ΔE is the increment in bonding energy, every time that the number of bonds is increased by one unit. Although this modelling is somewhat arbitrary (note that it is not valid for $n_i = 0$), it is the simplest way to generalize both the model of Eq. (2) where $\Delta E = 0$ and that considered in [1–3] where $E_0 = 0$. By changing simultaneously ΔE and E_0, it makes it possible to modify the hierarchy between the energies of an atom in the solid state according to its number of bonds, while keeping unchanged the whole equilibrium between the solid and the liquid. The detailed balance principle requires that

$$w_d(i) = w_c(i) \exp[-E(i)/k_B T]. \tag{4}$$

If one further assumes that the condensation rate constant remains independent of the condensation site, the dissolution rate at site i may be rewritten as

$$w_d(i) = w_d^0 \exp[-n_i \Delta E/k_B T], \tag{5}$$

where $w_d^0 = w_c \exp[-E_0/k_B T]$ includes the constant energy contribution. The equilibrium A concentration is obtained from the equality of the dissolution and condensation fluxes as

$$c_A^{eq} = \frac{w_d^0}{w_c} \left\langle \exp\left[-\frac{n_i \Delta E}{k_B T}\right] \right\rangle_{i \in S_{aged}}, \tag{6}$$

where the average is taken on the solid-solution interface of the aged sample (i.e., a long time after the saturation of the solution in A species).

Series of simulations have been made by changing in a correlated manner the ratios $\Delta E/k_B T$ and w_d^0/w_c so as to keep the equilibrium solubility nearly constant and equal to about 10^{-4}. Fig. 3 displays the morphologies of the aged samples and Table 1 summarises some char-

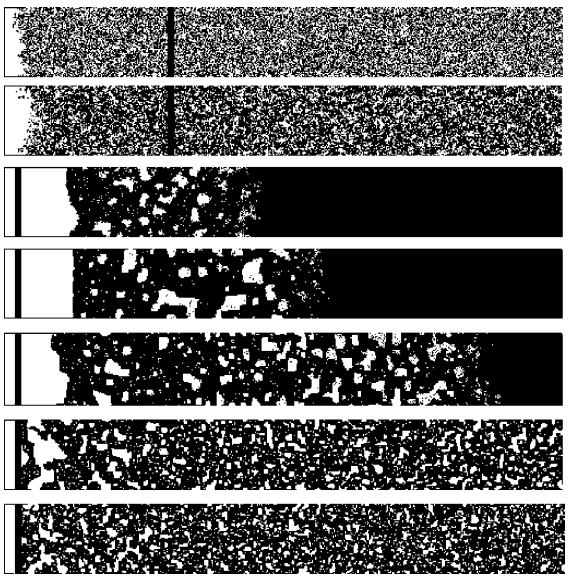

Fig. 3. Morphology of the aged gel for different values of $\Delta E/k_B T$ (from top to bottom: $\Delta E/k_B T = 0.0$, 0.7, 1.6, 2.3, 3.0, 3.9 and 4.6). The images correspond to longitudinal 64×512 cross-sections. The vertical lines represent the position of the initial free interface. The foam continue to grow in both directions in the two first pictures, while the gel is stabilized in the five others. All the simulations have been done with $p_B = 0.25$ and $S/V = 4 \times 10^{-6}$, the other parameters are given in Table 1.

Table 1
Characteristics of the aged gel for different values of $\Delta E/k_BT$

$\Delta E/k_BT$	w_d^0/w_c	c_A^{eq}	d_S	d_G	d_B
0.0	1.25×10^{-4}	1.7×10^{-4}	<0	infinite	infinite
0.7	1.00×10^{-3}	1.4×10^{-4}	<0	infinite	infinite
1.6	1.56×10^{-2}	1.2×10^{-4}	50	180	200
2.3	1.25×10^{-1}	1.2×10^{-4}	50	250	250
3.0	1.00	1.1×10^{-4}	15	440	380
3.9	15.6	0.8×10^{-4}	0	720	620
4.6	125	0.9×10^{-4}	0	890	750

The shrinkage depth d_S, the gel thickness d_G and the equivalent B species thickness d_B are expressed as numbers of single layers.

acteristic features of the altered sample in the final state: the equilibrium solubility c_A^{eq}, the shrinkage depth d_S, the thickness of the altered layer d_G and the equivalent thickness of dissolved B species d_B. The latter is defined by the relation $N_B = p_B \times S \times d_B$, where N_B is the total number of dissolved B atoms. First, it turns out that our objective to maintain a fixed solubility is almost reached. Second, one sees that d_B is equal to about 85% of $(d_S + d_G)$, which means that most of the soluble species have been removed from the altered layer, in agreement with the experimental practice to monitor glass leaching by recording the release of boron and alkalis in solution [10]. Finally and most importantly, one observes that changing $\Delta E/k_BT$ has dramatic consequences on both the morphology of the altered layer and the progress of the leaching. For $\Delta E/k_BT = 0.7$, one obtains the same result as for $\Delta E = 0$ (Fig. 1): a swollen gel with negative shrinkage and endless progression of the leaching front. The situation changes completely for $\Delta E/k_BT = 1.6$, where an altered monolithic layer is formed with a finite thickness (180 single layers, which corresponds to about 60 nm). The progress of the leaching front is stopped. The porosity is almost occluded and the typical pore size is of the order of 10–15 sites in width (i.e., 3–5 nm). When $\Delta E/k_BT$ is further increased, the general morphology remains the same, but (i) the shrinkage disappears progressively, (ii) the penetration depth increases and (iii) the pore size decreases.

Thus, the degree of alteration is not a monotonic function of $\Delta E/k_BT$. The sample is completely invaded when $\Delta E < k_BT$ because of the transformation of the sample in foam. Then, there is a minimum when ΔE is slightly larger than k_BT, since then all A atoms may be dissolved, whatever their environment is, and then redeposited to another place. As $\Delta E > k_BT$, dissolution-recondensation dynamics favour stronger (i.e., more connected) sites. This allows a complete reconstruction of the altered layer after the removal of the soluble B species and gives rise to an important ripening of the pore walls as observed in the third, fourth and fifth images in Fig. 3. The smaller the $\Delta E/k_BT$ (larger than 1), the easier the restructuring and the faster the blocking of the leaching. Finally, when $\Delta E/k_BT$ is further increased, it becomes very difficult to dissolve A atoms with a large number of neighbours (4 or 5 for the cubic lattice). This inhibits the shrinkage and the complete restructuring and delays the porosity occlusion, allowing a deeper penetration of alteration.

Two series of simulations have been performed as a function of the S/V ratio for $\Delta E/k_BT = 3.0$ and

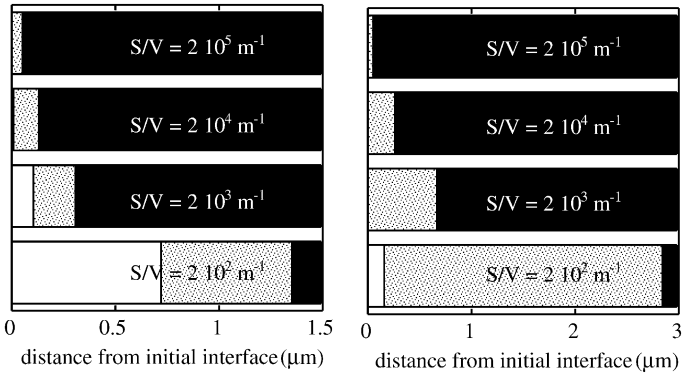

Fig. 4. Schematic views of the altered glass long after the saturation of the solution as a function of S/V for (left) $\Delta E/k_BT = 3.0$ and (right) $\Delta E/k_BT = 4.6$. The values of S/V as given in the pictures. The shrinkage zone is blank, the gel is grey and the unaltered glass is black. Note that the horizontal scale is different in the two pictures.

$\Delta E/k_BT = 4.6$. Fig. 4 shows schematic pictures of the altered aged systems in both cases. For convenience, the S/V ratio and the thicknesses have been converted into real-world units, using 0.2 and 0.3 nm as molecular sizes in the solution and in the solid state, respectively. One sees that the alteration depth, that we define as the sum of the shrinkage depth and the gel thickness, increases plainly as S/V decreases, typically from about 0.1 μm for high S/V ratios to a few μm for 200 m^{-1}. However, this increase is much less than the one expected for a regular layer-by-layer dissolution of the sample. In this case, the alteration depth would be equal to the shrinkage depth and directly proportional to the solution volume. There are two reasons for the difference. The first one is that the dissolution is selective: the weakest (i.e., the less connected) A species are dissolved in preference, and thus, one does not deal with a simple layer-by-layer dissolution. The second reason is that, even when the amount of dissolved A species is extremely weak (for example, the dissolution of three single layers is enough to reach the solubility saturation of 10^{-4} with $S/V = 2 \times 10^5$ m^{-1}), there is always a finite alteration layer, which is due to the initial departure of the soluble B species. This effect explains that the dissolution is less congruent and the $(S/V) \times t$ scaling less verified at high S/V ratios [1,8,9].

The main difference between the two situations displayed in Fig. 4 concerns the shrinkage. It is important for $\Delta E/k_BT = 3.0$, whereas the alteration is practically isovolumetric for $\Delta E/k_BT = 4.6$ even for a low S/V ratio of 200 m^{-1}. As a consequence, the density of A species is nearly the same in the gel and in the unaltered glass in the first case, while it is lower in the gel in the second one. The difference comes from the fact that some A elements become very difficult to dissolve when $\Delta E/k_BT$ is large. The same effect was observed when quasi-insoluble C species were introduced [1]. This shows again the importance of the $\Delta E/k_BT$ ratio for describing the alteration, but this provides also an indirect way to determine experimentally this factor by measuring the shrinkage depth or the gel density.

To conclude, we have shown that the gel morphology, the gel thickness, the shrinkage, and finally the protective or non-protective nature of the surface layer, are highly dependent on the dissolution-recondensation model, even when the glass solubility (silica concentration in solution) remains unchanged. The important factor is the graduation in the difficulty to remove particles (silicon atoms) with a higher number of neighbours. To simplify, we have introduced this graduation effect by defining ΔE as a constant difference in energy between sites with n and $n+1$ bonds, adjusting E_0(or w_d^0) to keep the solubility constant. There are other ways to reach the same object, for example, to make the energy in the solid state to depend more than linearly on the number of bonds. Moreover, the graduation in the difficulty to remove particles from the solid may also result from kinetic causes, such as the steric hindrance, which may reduce the accessibility of water to the sites with a large number of neighbours. To handle properly these effects would require us to use a more realistic lattice than the one considered in the present work.

References

[1] F. Devreux, P. Barboux, M. Filoche, B. Sapoval, J. Mater. Sci. 36 (2001) 1331.
[2] M. Aertsens, P. Van Iseghem, Mater. Res. Symp. Proc. 412 (1996) 271.
[3] M. Aertsens, Mater. Res. Symp. Proc. 556 (1999) 409.
[4] M. Aertsens, D. Ghaleb, these Proceedings, p. 37.
[5] B. Grambow, Mat. Res. Symp. Proc. 44 (1985) 15.
[6] E. Vernaz, J.L. Duchaussoy, Appl. Geochem. 1 (1992) 13.
[7] W.L. Ebert, J.J. Mazer, Mater. Res. Symp. Proc. 333 (1994) 27.
[8] X. Feng, I.L. Pegg, Y. Guo, A.A. Barkatt, P.C. Macebo, Mater. Res. Symp. Proc. 176 (1990) 383.
[9] T. Advocat, PhD thesis, Université Louis Pasteur, Strasbourg, 1991.
[10] B.E. Sheetz, W.P. Freeborn, D.K. Smith, C. Anderson, M. Zolensky, W.B. White, Mater. Res. Symp. Proc. 44 (1985) 129.